Ridgelet-Based Robust and Perceptual Watermarking for Images

Xiao Liang[†] , *Wei Zhihui* [††],*and Wu Huizhong*

Department of Computer Science, Nanjing University of Science & Technology, China, 210094

Summary
A watermarking algorithm operating in the ridgelet domain is proposed. Since the most significant coefficients of the ridgelet transform(RT) can represent the most energetic direction of an image with straight edge, the image is first partitioned into small blocks and RT is applied for each block. According to the structure of ridgelet decomposition which perfectly match the multi-channel structure of the human visual system (HVS), a Just Noticeable Distortion(JND) is accomplished by pixel by pixel taking into account the contrast sensitivity, frequency sensitivity and masking effect of all ridgelet subbands. The watermark consists of a pseudorandom sequence which is adaptively added to the most significant ridgelet coefficients of each image block, the strength of embedding watermark is adjust by the JND. As usual, the watermarks are blindly detected using a correlation detector. The detection threshold is chosen by the statistical properties of the correlation detector. Experimental results show that the robustness and transparency can be well proved by the proposed watermarking algorithm.

Key words:
Information security; digital watermark; ridgelet transform; perceptual embedding; blindly detection

1. Introduction

In the last decade, much extensive attention has been paid to digital watermarking for images, video and audio, because it give a novel solution for the copyright protection of digital media. The image watermarking algorithms can be classified into two groups depending on the domain of watermarking embedding, i.e. the spatial and the frequency-domain. It is widely accepted that the frequency-domain watermarking algorithms can easily exploit the perceptual models based on characteristics of the Human Visual System (HVS) to achieve the best tradeoff between imperceptibility and robustness to image processing, and also easy to be implemented in compressed domain. Hence many algorithms have been developed in DCT or wavelet domain [1][2].

In this paper, we propose a novel image watermarking based on a recently introduced family of transform-the ridgelet transform (RT)[3]. The RT uses basis elements which exhibit high directional sensitivity and are highly anisotropic. The RT allows obtaining a sparse image representation where the most significant coefficients represent the most energetic direction of an image with straight edges. Hence, the block splitting process is introduced to deal with the straight singularity and analyze the texture properties. Furthermore, compared with the multi-channel structure of the HVS, it is found that this multi-channel structure is perfectly matched by the pyramids structure of ridgelet decomposition. Hence, we establish a Just Noticeable Distortion(JND) by pixel by pixel taking into account the contrast sensitivity, frequency sensitivity and masking effect of all ridgelet subbands. Finally the watermarks are adaptively embedded in the most visual significant ridgelet coefficients according to the JND profile.

2. Ridgelet transform

2.1 Continuous ridgelet transform

Let us briefly review the 2-D continuous ridgelet transform in R^2 can be defined Candes E.J [4]. We pick a smooth univariate $\psi: R->R$ with sufficient decay and satisfying the admissibility condition

$$\int \left| \hat{\psi}(\xi) \right|^2 / |\xi|^2 < \infty \qquad (1)$$

which holds if, say, ψ has a vanishing mean $\int \psi(t)dt = 0$. Foe each $a > 0$, each $b \in R$ and each $\theta \in [0,2\pi)$, the bivariate ridgelet $\psi_{a,b,\theta} : R^2 \to R^2$ is defined by

$$\psi_{a,b,\theta}(x) = a^{-1/2} \cdot \psi((x_1 \cos\theta + x_2 \sin\theta - b)/a) \qquad (2)$$

This so called ridgelets are constant along ridge lines $x_1 \cos\theta + x_2 \sin\theta$, and along the orthogonal direction they are wavelets. Given an integrable bivariate function $f(x)$, we define its ridgelet coefficients by

$$R_f(a,b,\theta) = \int \psi_{a,b,\theta}(x) f(x) dx. \qquad (3)$$

A basic tool for calculating ridgelet coefficients is to view ridgelet analysis as a form of wavelet analysis in Radon domain. More precisely, denote the Radon transform as

Manuscript received February 25, 2006.
Manuscript revised February 28, 2006.

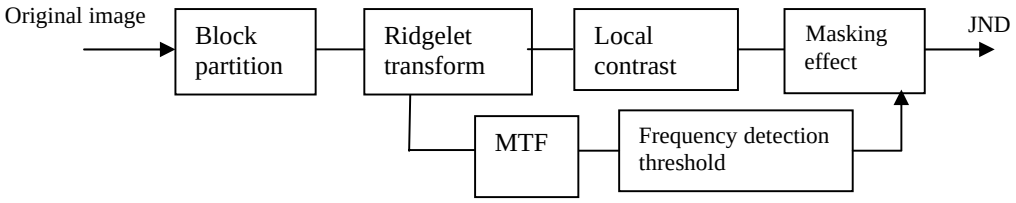

Fig.1. Proposed JND system in ridgelet domain

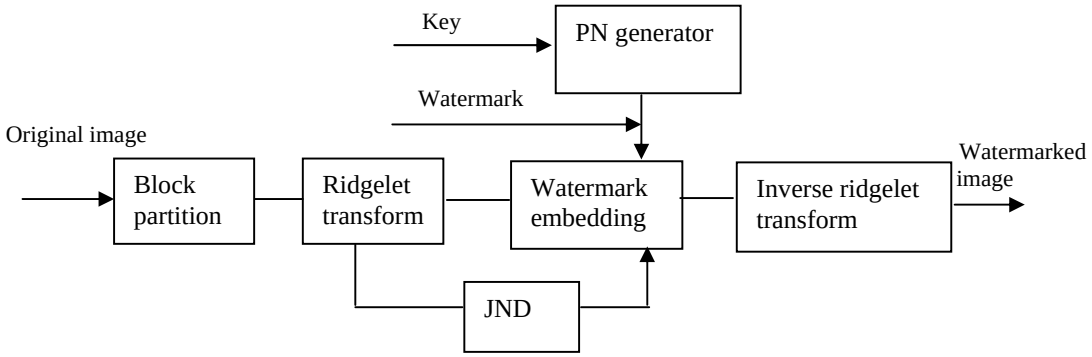

Fig.2. Proposed watermarking system

$$RA_f(\theta,t)=\int_{R^2} f(x)\delta(x_1\cos\theta+x_2\sin\theta-t)dx \quad (4)$$

then the ridgelet transform is precisely the application of a 1-D wavelet transform to the slice of the Radon transform.

$$R_f(a,b,\theta)=\int \psi_{a,b}(t)RA_f(\theta,t)dt. \quad (5)$$

2.2. Digital ridgelet transform

In [5], a finite Radon transform (FRAT) is introduced. The FRAT of a real function I defined on a finite grid Z_p^2, being $Z_p=\{0,1,2.....p-1\}$ where p is a prime number, is

$$r_k[l]=FRAT_I(k,l)=\frac{1}{\sqrt{p}}\sum_{(i,j)\in L_{k,l}} f[i,j]$$

$L_{k,l}$ Defines the set of points that form a line on the lattice Z_p^2. Specifically

$$L_{k,l}=\{(i,j): j=ki+l(\text{mod } p), i\in Z_p\}$$

$$L_{p,l}=\{(l,j): j\in Z_p\}$$

being $0\le k<p$ the line direction (where $k=p$ corresponds to the vertical line) and l its intercept. In [8], it has been demonstrated that FRAT is invertible, thus providing a representation for a generic image. The invertible finite $IFRAT_I[k,q]$, with $q\in Z_p$, is obtained by taking the 1-D discrete wavelet transform on each FRAT projection sequence $r_k[0],r_k[1],....r_k[p-1]$, for each direction k.

3. Proposed Watermarking System

In order to perform the watermark embedding procedure in perceptual mode, it is need to establish the JND system in ridgelet domain employing the visual properties of HVS (see Fig.1). The block diagram of our perceptually based digital watermarking technique is shown in Figure2. First, the original image $I(x,y)$ is split into non-overlapped blocks. Then, the block image is decomposed by digital ridgelet transform. And we estimate the JND profile in ridgelet transform domain and insert watermark in ridgelet coefficients according the JND profile. Finally, the watermarked image is obtained by inverse ridgelet transform.

3.1 Block Partitioning and classification

Assume the original image $I(x,y)$ is split into non-overlapped blocks of $N\times N$ denoted $B_l, l=0,1,2..B-1$

That is

$$I(x,y)=\bigcup_l B_l=\bigcup_l I^l(x',y'),0\le x',y'\le N$$

In an image, the different blocks usually have different features. The feature will affect the visibility of superimposed watermark signals. To embed watermarks as

Manuscript received February 25, 2006.
Manuscript revised February 28, 2006.

strongly as possible, we classified all blocks into two categories: S1 with weak texture, and S2 with stronger texture. The strength of watermark components embedded into block S1 should be weaker than that embedded into block in S2. Since HVS is more sensitive to a gray-level change in the block S1 than in the block S2. On the other hand, a block in S2 permits stronger watermark component to be inserted.

The classification is based on edge point density[6]. That is $B_l \in S_1$ if

$$number\{e(x,y) \neq 0, (x,y) \in B_l\} \leq T_1$$

where $number\{p\}$ denotes the number of points satisfying the condition by p ; $e(x,y)$ is a binary edge map of $I(x,y)$ obtained by applying a gradient operator followed by a threshold T_1 is a preset criterion. Otherwise, $B_l \in S_2$.

3.2. Ridgelet subband grouping

In the folowing we will represent the ridgelet coefficients by means of a suitable subband division to match the muti-channel processing mechanism of HVS. Since ridgelet transform can be viewed as wavelet analysis in randon domain, in the one-dimensional wavelets case, ridgelet divides frequency domain into a certain dyadic segments, while in the multi-dimensional wavelets case, ridgelet divides the domain into dyadic coronae. As shown in fig. 3, the circular rings $\{\omega : 2^j \leq |\omega| \leq 2^{j+1}\}$ with the same center are partitioned according to the orientations of ridgelets, each block is the localized domain of a certain ridgelet, and the number of these domains becomes larger with the increasing scale.

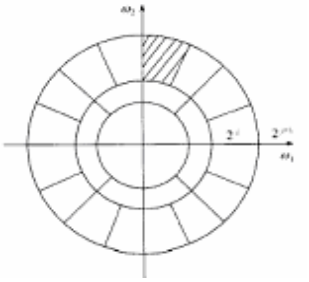

Fig3. Ridgelet subbands division

For our watermarking system, only one-dimensional wavelet transform is needed to apply in radon domain. Let $\mathrm{I}_{\omega,\theta}$ be ridgelet coefficients, where ω denotes the frequency parameter while θ denotes the angular parameter. Coefficients with the same spectral indices can be grouped together to form a subband.

Then all the ridgelet coefficients in,

$$\Omega_m^k = (2^{m-1}, 2^m) \times (\frac{k\pi}{2^m}, \frac{(k+1)\pi}{2^m})$$

are grouped together into a subband denoted by $\mathrm{I}_{\omega,\theta} = I_{m,k} = \{I_{m,k}(i,j)\}$, where

<table>
<tr><td colspan="8">$I_{0,0}$</td></tr>
<tr><td colspan="4">$I_{1,0}$</td><td colspan="4">$I_{1,1}$</td></tr>
<tr><td colspan="2">$I_{2,0}$</td><td colspan="2">$I_{2,1}$</td><td colspan="2">$I_{2,2}$</td><td colspan="2">$I_{2,3}$</td></tr>
<tr><td>$I_{3,0}$</td><td>$I_{3,1}$</td><td>$I_{3,2}$</td><td>$I_{3,3}$</td><td>$I_{3,4}$</td><td>$I_{3,5}$</td><td>$I_{3,6}$</td><td>$I_{3,7}$</td></tr>
</table>

Fig.4. Ridgelet subbands grouping

$$\omega = \sum_{l=0}^{m} 2^l + i, \theta = \frac{k\pi}{2^m} + j. \quad (7)$$

and $m = 0,1,..L \quad k = 0,\cdots,2^m - 1.$

If for each block B_l , DRT transform is applied then the ridgelet subband coefficients can be denoted by

$$\left\{I_{m,k}^l(i,j)\right\} = DRT\{I_l(x',y')\}$$

3.3. Perceptual model in ridgelet domain

In this section, we will consider to constructing the ridgelet-based perceptual model for computing the just noticeable distortion for each ridgelet coefficient. Figure 2 shows the procedures for the computing JND thresholds. The proposed JND profile of a still image depends on the spatial frequency sensitivity, the sensitivity to local gray contrast and texture masking[7][8]:

1) The spatial frequency sensitivity is so-called modulation transfer function (MTF), which provides relative tolerance of the HVS to noise at different spatial frequencies and different orientations.

2) The eye is less sensitive to noise in those areas of the image where brightness is high.

3) The eye is less sensitive to noise in the highly textured areas of the image.

Then the JND profile of $I_{m,k}^l(i,j)$ is function of local Image properties, such as local background luminance and $I_{0,0}^l\left(\left\lfloor \frac{i}{2^m} \right\rfloor + 1, j\right)$ and the frequency detection threshold of subband image Ω_m^k .

Firstly, since human visual sensitivity to luminance patterns is reduced as the mean local luminance is increased, the thresholds are related to the local contrast. Generally, physical contrast is defined by Weber contrast.

However, the definition only quantifies the global characteristics of images, and can not be used to describe the complex image. In this paper, we define the contrast in ridgelet transform domain by modifying the definition of "local band limited contrast" proposed by Daly [9].

For subband image $I^{l}_{m,k}$ ($m=0,1,2,3$ $k=0,\cdots,2^{m}-1$), the local contrast in ridgelet domain is defined by

$$C^{l}_{m,k}(i,j)=\frac{\left|I^{l}_{m,k}(i,j)\right|}{I^{l}_{0,0}\left(\left\lfloor\frac{i}{2^{m}}\right\rfloor+1,\ j\right)^{\lambda}}\quad,\qquad m\geq 1 \tag{8}$$

with some constant λ.

Secondly, according to the research of A. Vassilev [10],the modulation transfer function(MTF) describes the variations in visual sensitivity as a function of spatial frequency. In general, MTF models the visual sensitivity as a function of radial spatial frequency, orientation in degree, light adaptation, image size in visual degree, lens accommodation and eccentricity in degrees. In this paper, we simplify the MTF as the function of the first two parameters: radial spatial frequency ω , orientation in degree θ,

$$\mathrm{M}TF(\omega,\theta)=\min\left[S\left(\frac{1.24\omega}{1.5(0.15\cos(4\theta)+0.85)}\right),\ \ S(\omega)\right] \tag{9}$$

Here

$$S(\omega)=0.72((3.23(25\omega^{2})^{-0.3})^{5}+1)^{-0.2}\cdot\omega\cdot e^{-0.33\omega}\sqrt{1+0.06e^{0.33\omega}} \tag{10}$$

Then frequency detection threshold of subband image $I^{l}_{m,k}$ is determined by

$$T^{k}_{m}=\frac{\iint_{\Omega^{k}_{m}}\omega\ d\ \omega\ d\ \theta}{\iint_{\Omega^{k}_{m}}MTF\ \ (\omega\ ,\theta\ )\omega\ d\ \omega\ d\ \theta}. \tag{11}$$

Since the above formula is independent of the image content, the frequency detection threshold can be calculated in advance to reduce the computation complexity. Figure 4 shows the result of each subband image.

Finally, based on the masking function model made by Scott Daly, the JND profile of $I^{k}_{m}(i,j)$ is given by

$$JND(I^{l}_{m,k}(i,j))=T^{k}_{m}\cdot\left(1+\left(0.0153\left(392.498\cdot\left|\frac{C^{l}_{m,k}(i,j)}{T^{k}_{m}}\right|\right)^{\gamma}\right)^{4}\right)^{1/4} \tag{12}$$

where γ is a binary value function of texture properties of $I^{l}_{m,k}(i,j)$ in the block B_l given by

$$\gamma(I^{l}_{m,k}(i,j))=\begin{cases}1, & if\quad B_l\in S1\\ 0.7 & if\quad B_l\in S2\end{cases}$$

Our visibility threshold model combines the frequency detection threshold and the masking effect of HVS.

3.4. Watermark Generation

In our watermarking system, the meaningful signature such as the logo of the image owner or the information related to the host image such as owner's name, image ID, etc is chosen to generate the embedding signal. The embedding signal $L=[l_1,l_2,...l_{N_w}]$ with $l_i\in\{0,1\}$ is a bit sequence with length N_w. We modulate the bit sequence by a bit-wise logical XOR operation with a pseudorandom with sequence $PN=[s_1,s_2,...s_{N_w}]$ with $s_i\in[0,1]$ to give the watermark sequence $W=[w_1,w_2,...w_{N_w}]$ by $w_i=s_i\otimes l_i$

3.5. Watermark Embedding

Given the B_l block image, the digital ridgelet transform is applied and ridgelet subband grouped to obtain the subband coefficients $I^{l}_{m,k}(i,j)$,the $JND(I^{l}_{m,k}(i,j))$ is also calculated. We divide the ridgelet coefficients into separate groups, in each of which the watermark noise with different energy is inserted and its energy is controlled by ridgelet coefficients so that watermark noise does not exceed the JND of each ridgelet coefficient.

Assume that we divide the ridgelet coefficient into M groups $\{X^{l}_{i}\},i=1,2...M$

$$X^{l}_{i}=\{I^{l}_{m,k}(s,t)\,|\,q_{i-1}<\left|I^{l}_{m,k}(s,t)\right|<q_i,m=0,1,2,3\ \ k=0,\cdots,2^{m}-1\} \tag{13}$$

where $q_i(i=1,2...M)$ are some given constants, and satisfy

$$q_0<q_1<\cdots<q_M=\max\{I^{l}_{m,k}(s,t)\}$$

in our approach, each group X_i has its energy factors g^{l}_{i} of the watermark noise inserted in this group, which determinate by

$$g^{l}_{i}=JND(q_{i-1})$$

where JND function is given in ().Hence for $I^{l}_{m,k}(s,t)\in X^{l}_{i}$,the watermark noise is $g_i\cdot w_l$. Then the watermark is superimposed into each ridgelet coefficients in X^{l}_{i}

$$\bar{I}^{l}_{m,k}(s,t)=I^{l}_{m,k}(s,t)+\alpha\cdot f(I^{l}_{m,k}(s,t))w^{l}_{m,k}(s,t) \tag{14}$$

where $f(I^l_{m,k}(s,t))$ is piecewise function of $I^l_{m,k}(s,t)$ given by

$$f(I^l_{m,k}(s,t)) = \begin{cases} g_i & if \quad I^l_{m,k}(s,t) \in X^l_i \\ 0 & otherwise \end{cases}$$

and $w^l_{m,k}(s,t)$ is the watermark signal generated in Section 3.2. The parameter α is a scaling factor, is adjustable by user to increase (or) decrease the protected image fidelity and decrease (or increase) the security of watermark protection at the same time.

As given in (14), the error introduced by watermark casting is

$$e^l_{m,k}(i,j) = \alpha \cdot f(I^l_{m,k}(s,t)) w^l_{m,k}(s,t)$$

given $|w^k_m(i,j)| \le 1.0$, the mean square error(MSE) introduce by the watermark can be computed as:

$$MSE \le \frac{\sum_{l=1}^{B} \sum_{m,k} \sum_{(i,j)\in\Omega^k_m} \left(\alpha \cdot f(I^l_{m,k}(i,j))\right)^2}{N_W},$$

where N_W is the length of the embedded watermark sequence. Let $T_{\max}$ denotes the maximum JND of all ridgelet coefficients. Since only N_w significant coefficients are selected for watermark insertion, thus, we have:

$$MSE \le \alpha^2 (T_{\max})^2,$$

Thus, the value of α is limited by the following,

$$\alpha \le \frac{1}{T_{\max}} \sqrt{MSE}$$

3.6. Invisible watermark detection and extraction

When the protected image is distributed to the public, the exact location of selected significant coefficients and the amount of the cast watermark should be unknown to attackers so that the watermarks cannot be removed easily under various attacks. Possible attacks include linear or nonlinear filtering, addition of Gaussian or non-Gaussian noise, image enhancements, re-sampling or re-quantization, and image compression, etc.

Let I^* denote an attacked image with a certain type of attack, then the similarity between I^* and W is defined as

$$\rho = \frac{1}{N_w} \sum_{l=1}^{B} \sum_{(m,k)} \sum_{(i,j)} I^{*l}_{m,k}(i,j) \cdot w^l_{m,k}(i,j),$$

can be used to determine whether a given mark is presented or not, by simply comparing it to a predefined threshold.

In some application, the embedded watermark image may be hoped to extract for resolving rightful ownership. In our watermark decoding system, the watermark data extraction process is accomplished by using the watermarked image, and the seeds used by the pseudo-random generation mechanism in the watermarks embedding step. First, apply the same ridgelet transform to the watermarked image and then obtain the N_w significant coefficients selected for watermark embedding. Then an inverse procedure similar with embedding equation (14) is applied to get the watermark bit. Finally the obtained watermark signals are used to recover the original watermark image.

3.5. Statistical analysis for threshold selection

It is important for a correct behavior of the watermark detection system, to properly choose the decision threshold. In the practical watermark decoder, only one of the following situations is possible:

Hp.0: the image is not marked with *W*;

Hp.1: the image is marked with *W*.

To discriminate between Hp.0 and Hp.1, the detector computes ρ and compares it with a threshold T_ρ, if ρ is lower than T_ρ then the decoder decides the image is not marked with *W*, whereas if ρ is higher than the threshold, the decoder assumes the image is marked with *W*. To determine the value of T_ρ, the detector error can be take into account the error probability of deciding for the wrong hypothesis, written as:

$$P_E = P(1|0) \cdot P(0) + P(0|1) \cdot P(1)$$
$$= P(\rho > T_\rho|0)P(0) + P(\rho < T_\rho|1)P(1)$$

where $P(0)$ and $P(1)$ is a prior probability of Hp.0 and Hp.1, $P(\rho < T_\rho|1)$ is the probability of missing the presence of the mark (false negative) and $P(\rho > T_\rho|0)$ the probability of revealing the presence of *W* when *W* is not actually present (false positive).

To apply statistical decision theory, some assumptions must be made on the random variables forming the observation variable ρ. We know that $w^l_{m,k}(i,j)$'s are binary valued, zero mean, independent random variables. Besides, they do not depend on ridgelet coefficients. As to $\bar{I}^l_{m,k}(i,j)$'s, we make the realistic assumption that they are zero mean, independent variables. By exploiting the central limit theorem, we can also assume that is normally distributed. Let us denote the mean value and the variance of ρ on the

above hypothesis of Hp.0 and Hp.1 are $\mu_{\rho_0}, \mu_{\rho_1}$ and $\sigma_{\rho_0}, \sigma_{\rho_1}$ respectively, then they can be evaluated in the following:

$$\mu_{\rho 0} = 0;$$

$$\mu_{\rho 1} = \frac{\alpha}{N_W} \sum_{l=1}^{B} \sum_{(m,k)} \sum_{(i,j) \in I_m^k} E\left(f(I^l_{m,k}(i,j))\right) ;;$$

$$\sigma^2_{\rho 0} \approx \frac{\sigma^2_w}{(N_W)^2} \sum_{l=1}^{B} \sum_{(m,k)} \sum_{(i,j) \in \tilde{I}_m^k} E\left(I^l_{m,k}(i,j)\right)^2$$

$$\sigma^2_{\rho 1} \approx \frac{\sigma^2_w}{(N_W)^2} \sum_{l=1}^{B} \sum_{(m,k)} \sum_{(i,j) \in \tilde{I}_m^k} \left(\tilde{I}^l_{m,k}(i,j)\right)^2 .$$

Thus we assume that:

$$P\left(\rho > T_\rho \mid 0\right) = \frac{1}{2} erfc\left(\frac{T_\rho}{\sqrt{2\sigma^2_{\rho_1}}}\right)$$

and by imposing that $P\left(\rho > T_\rho \mid 0\right) \le 10^{-8}$ it is obtained

$$T_\rho = 3.97 \sqrt{2\sigma^2_{\rho 1}}$$

4. Experimental results

The proposed watermarking algorithm has been tested on many standard images such as "Baboon", "Lena", "Peppers", "Mandrill" etc with size of 510×510. They have been partitioned into blocks of $N \times N$ pixels with $N = 17$, this obtaining $B = 900$ blocks. A watermark composed by $N_w = 900$ bit generated by the method in Section 3.4 using a binary watermark logo of 30×30 pixels. In the following, we will only give the results regarding the 512×512 8-bit standard image "Lena". Fig.6 shows the original image, watermarked images with PSNR=39.34dB and the absolute difference between of them. It is clearly see that the imperceptibility of the embedded watermarks, because of them are mainly hidden into high activity regions and around edges which guaranteed by the JND model and the parameter $\alpha = 0.40$.

The robustness of the proposed watermarking algorithm is tested against the attack from anti-watermark program such as UnZign and StirMark[11]. For the attacks of the software, we compute the response of ρ_T of the watermark detector to 1000 watermarks randomly generated. Experimental results show that the detector provides a correlation value far higher than the threshold T_ρ only for the actual embedded watermark out of the 1000 tested: JPEG compression, noise superimposed, cropping and twisting processing, etc.

Take the attack of JPEG compression for example, In Fig. 5, the response of the detector to the watermarked image is plotted against JPEG compression with increasing quality factor of the image (from 40% to 90%), along with the detection threshold, and the second highest response of the detector (i.e., the highest response among those produced by the detector when the 999 fake watermarks are tested). The detector response is always higher than the threshold. The second highest detector response always stays below the threshold.

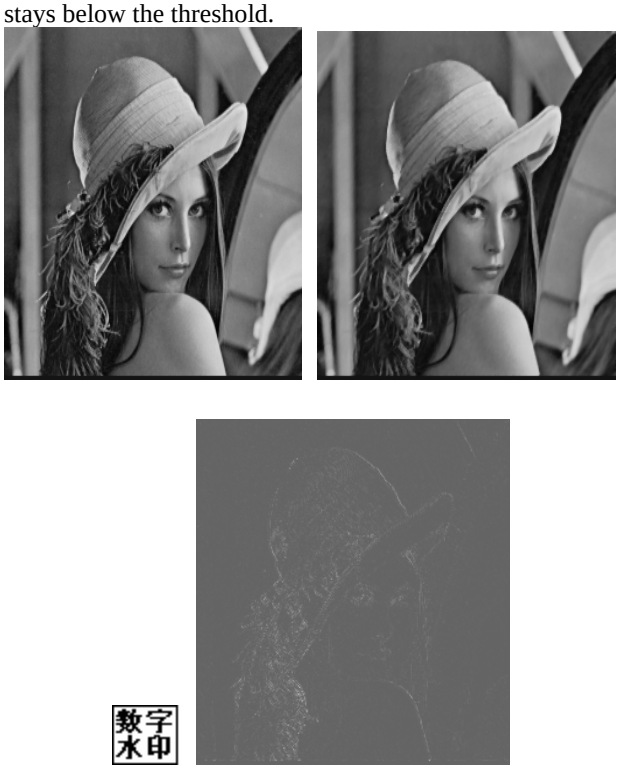

Fig,4. Up-left: the original Lena image. Up-right: watermarked image. Bottom left: the embedding logo. Bottom right: absolute difference between the original image and the watermarked one, magnified by a factor 6.

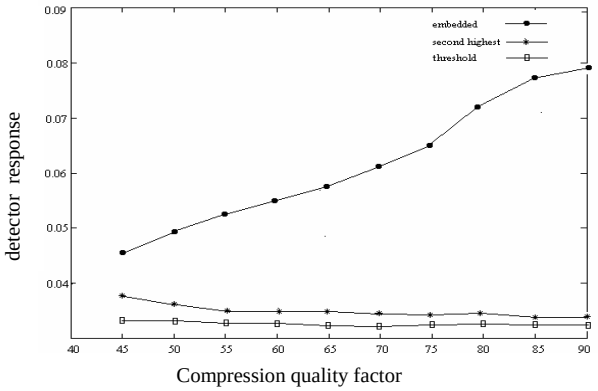

Fig. 5. Plot of the response of the correlation based detector to the embedded watermark (ball marker), the second highest detector response (diamond markers), and of the threshold (square markers), corresponding

to JPEG compression with increasing quality factor. 1000 marks were tested.

We also take an investigation on the robustness test of the watermarked image against cropping attack, low-pass filtering, subsampling, addition of noise, etc. For "Lena" image, after mean filtering, clipping to a quarter (lost 75% of the watermarked image), or 2 : 1 subsampling along both horizontal and vertical directions in the watermarked image, the responses of the correlation based detector are 0.065, 0.054, and 0.073,respectively, all well above the threshold. Figure 6 shows the result of the watermark logo extracted from the embedded "Lena" after some clipping operation, while Figure 7 show the plot of the response of the detector to the embedded watermark when the 999 fake watermarks are tested with the same cropping area in Fig.6.

Experimental results also show that better robustness performance can be obtained for the images with more complex texture, for example "Baboon" image.

Figure 6. Up-left: watermarked image "Lena" after a cropping distortion and the extracted watermark logo.

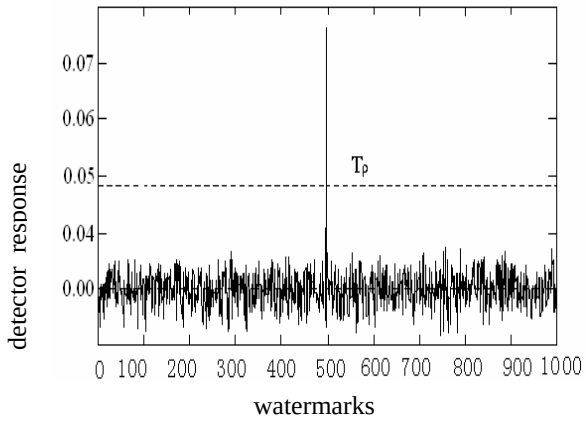

Figure 7. Detector response for the watermarked "Lena" with same cropping area in Fig.6.

5. Conclusions

In this paper, a perceptually based watermarking algorithm in ridgelet domain is proposed. Based on the principle of multi-channel decomposition of ridgelet transform, HVS properties are exploiting to estimate the JND profile. Then watermark casting scheme which searches the perceptually significant ridgelet coefficients. The watermark sequence is cast into the selected coefficients to provide a higher tolerance to various attacks. Moreover, the fidelity of the protected image can be adjusted by using the weighting factor α of the casting watermark energy.

Acknowledgements

This work was supported by the Youth Talent Foundation of Nanjing university of science and technology No.NJUST200401 and the National Special Foundation of Doctoral Programs Grant No. 20020288024 (in Chinese).

References

[1] I. J. Cox, J. Kilian, F. T. Leighton, and T. Shamoon, "Secure spread spectrum watermarking for multimedia," *IEEE Trans. Image Processing*, vol.6, pp. 1673–1687, Dec. 1997.

[2] B.Mauro, P.Alessandro, "Improved wavelet-based watermarking through pixel-wise masking", *IEEE Transactions on image processing*, vol.10, no.5, pp.783-791,2001.

[3] M. N. Do and M. Vetterli, "The finite ridgelet transform for image representation", *IEEE Trans. Image Processing*, vol. 12, pp. 16–28, Jan. 2003.

[4] E.J.Candès,, "Ridgelets: Theory and application," Ph.D. dissertation, Department Statistics, Stanford Univ., CA,1998.

[5] J.-L. Starck, E. J. Candès, and D. L. Donoho, "The curvelet transform for image denoising," *IEEE Trans. Image Processing*, vol. 11, pp. 670–684,June 2002.

[6] Jiwu Huang, Yun Q.Shi, and Yi Shi. Embedding image watermarks in DC components. *IEEE Transaction on circuits and system for video technology*,vol.10, no.6, pp.974-979,2000.

[7] I. Podilchuk, W. Zeng, "Image-adaptive watermarking using visual models", *IEEE Journal on Special Areas in Communications*, vol 16, no.4, pp. 525-539, 1998.

[8] Zhihui Wei, Q.Peng, etal. "Perceptual digital watermark of images using wavelet transform," *IEEE Transaction on Consumer Electronics*, vol.44, No.4, pp. 1267~1272,1998.

[9] S.Daly "The visible differences predictor: An algorithm for the assessment of image fidelity", *SPIE, Human Visual Processing, and Digital Display*, vol.1666,No.3, pp.2-15,1992,.

[10] A. Vassilev, "Contrast sensitivity near borders significance of test stimulus: Form, size, and duration", *Vision Research*, vol. 13, no.11, pp.719~730,1973.
[11] R.J.A Fabien, M.G Kuhn, "Attacks on copyright marking systems", *In second workshop on information Hiding*, Portland, Oregon, April 15~17,1998.

Xiao Liang, was born Hunan province of China in 1976, received the B.S. and M.S. degrees in applied mathematics, and received the Ph.D. degree from Nanjing University of Science and Technology, China in 2004. He is a lecture at school of computer science. His current research interests include information hiding, digital watermarking and image coding. He has published more than 30 papers on these topics in journals and conferences.

Wei Zhihui, was born Jiangsu province of China in 1963, received Ph.D degree from South East University of China in 2001. Now he is professor of Nanjing University of Science and Technology. His main research contributions include video and image coding, watermarking and steganography, speech and audio processing. He has published more than 40 papers on these topics in international journals and conferences.

Wu Huizhong, was born Shang hai province of China in 1942, professor, Ph.D. supervisor. His research activity is focused on multimedia systems, digital image processing, digital watermarking, and secure communication protocols, virtual reality, computer graphics and image theory. She has published more than 100 papers on these topics in journals and conferences.